IEEE Access
Multidisciplinary | Rapid Review | Open Access Journal

Received April 18, 2017, accepted May 24, 2017, date of publication June 13, 2017, date of current version July 17, 2017.

*Digital Object Identifier 10.1109/ACCESS.2017.2715280*

# 3-D Geometrical Model for Multi-Polarized MIMO Systems

**XUDONG CHENG[1], YEJUN HE[1], (Senior Member, IEEE), AND MOHSEN GUIZANI[2], (Fellow, IEEE)**

[1]Shenzhen Key Laboratory of Antennas and Propagation, College of Information Engineering, Shenzhen University, Shenzhen 518060, China
[2]Electrical and Computer Engineering Department, University of Idaho, Moscow ID 83844, USA

Corresponding author: Yejun He (heyejun@126.com)

This work was supported in part by the National Natural Science Foundation of China under Grant 61372077, in part by the Science and Technology Innovation Commission of Shenzhen under Grant ZDSYS 201507031550105, and in part by Guangdong Provincial Science and Technology Programs under Grant 2013B090200011 and Grant 2016B090918080.

**ABSTRACT** Multiple-input multiple-output (MIMO) systems capacity is highly influenced by the correlation between antennas, and the high correlation will result in a low capacity. Therefore, the multi-polarized antennas have been implemented in MIMO systems to reduce the correlation between antennas and realize the space efficiency. To better understand the performance of multi-polarized MIMO systems, polarization channel modeling is of great importance. In this paper, we establish a 3-D geometrical model for multi-polarized MIMO systems. Antenna cross-polar isolation (XPI), channel cross-polarization discrimination (XPD) and antenna tilt parameters have been considered in our model. The correlation and capacity of multi-polarized MIMO systems are analyzed, and we find that the XPI, XPD, and antenna tilt have an effect on the correlation and capacity simultaneously, which cannot be analyzed separately. Also, we compare our model with the existing measurements for validation, which shows that the proposed model is well in agreement with the measurements. Finally, we compare the performance of multi-polarized MIMO systems with the traditional uni-polarized MIMO systems, which shows that the performance of multi-polarized MIMO systems have robustness to the communication environment, and multi-polarized MIMO systems outperform uni-polarized MIMO systems in many communication scenarios.

**INDEX TERMS** MIMO, multi-polarized antennas, polarization, channel modeling, XPD.

## I. INTRODUCTION

Multiple-input multiple-output (MIMO) systems have yielded high capacity in wireless communication. While one major issue of MIMO systems is that the capacity is highly influenced by the correlation between antennas, and the high correlation between antennas results in a low capacity. An antenna spacing of at least half a wavelength at the user equipments and ten wavelengths at the base station (BS) are typically required for achieving a significant MIMO gain [1]. As the number of antennas increases to a large scale antenna array, it may not be achieved easily because of the space and size restrictions. Therefore, the multi-polarized antennas have been implemented in MIMO systems to reduce the correlation between antennas and realize the space efficiency. Also, it has been shown that the implementation of polarization for spatial multiplexing-based MIMO systems can lead to significant performance improvements [2].

To better understand the performance of multi-polarized MIMO systems as compared to the traditional uni-polarized MIMO systems (i.e., all the antennas have the same polarization directions), polarization channel modeling is of great importance. Polarization channel modeling is difficult because of the complexity of the polarization characteristics. Reflections, diffractions and scattering [3]–[5] of the electromagnetic signal in the wireless channel may result in channel depolarization, which means the polarization orientation may rotate or change after passing through the wireless channel [6]. A general method to measure the channel depolarization is to use the cross-polarization discrimination (XPD), which is defined as the ratio of the average received power in the co-polarized channel to the average received power in the cross-polarized channel [7]. Kwon and Stüber provided a geometric theory for channel depolarization and provided a mechanism for calculating

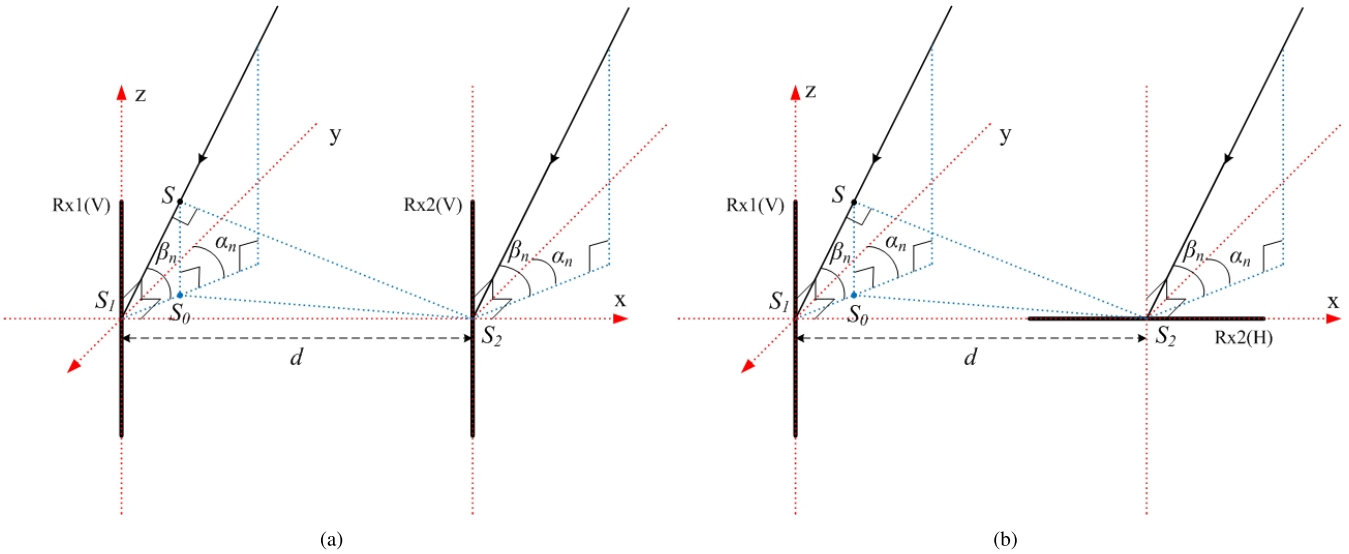


**FIGURE 1.** (a) 3-D uni-polarized MIMO systems transmission scenario. (b) 3-D multi-polarized MIMO systems transmission scenario.

XPD based on the locations of the scatterers [8]. While [7], [9], [10] proposed 3-D sphere geometrical models for polarized channels, which are somewhat complex and only have theoretical simulations without comparison with measurements. Other references [2], [11]–[14] modeled the multi-polarized MIMO systems channel as a Ricean fading channel, such that the channel matrix is composed of a line-of-sight (LoS) part and a scattering or non-line-of-sight (NLoS) part. They focused on just one factor such as the XPD, antenna cross-polar isolation (XPI) or antenna tilt. Many experiments in [15]–[19] have been carried out and measurements of multi-polarized MIMO systems from 2 GHz to 3.5 GHz were presented. While carrying out experiments is expensive and time-consuming, and some particular parameters are difficult to measure.

Although many researchers have considered polarization channel modeling, most of them focused on just one factor and considered the three factors separately. Actually, XPI, XPD and antenna tilt will happen simultaneously in the system link, and they have effect on the system link performance simultaneously, which can not be analyzed separately. In this paper, we propose a 3-D geometrical model for multi-polarized MIMO systems, and both the azimuth angles of arrival (AAoAs) and elevation angles of arrival (EAoAs) have been taken into account. The multi-polarized MIMO systems channel is modeled as a Ricean fading channel, and we consider antenna XPI, channel XPD and antenna tilt simultaneously. The correlation between multi-polarized antennas and the system capacity are analyzed. XPI, XPD and antenna tilt have effect on the correlation and system capacity simultaneously, which can not be analyzed separately. We compare our model with the existing measurements for validation, which shows the proposed model is well in agreement with the measurements. Also, we compare the performance of multi-polarized MIMO systems with uni-polarized MIMO systems in different communication scenarios, and it is found that the performance of multi-polarized MIMO systems have robustness to the change of antenna spacing, XPD, antenna tilt and etc. Finally, we summarize the comparison between the multi-polarized MIMO systems and uni-polarized MIMO systems in different communication scenarios to help choosing the suitable MIMO systems in different communication scenarios.

The remainder of this paper is organized as follows. Section II analyzes the correlation between multi-polarized antennas by considering XPI, XPD and antenna tilt. In Section III, the multi-polarized MIMO systems channel model is formulated and compared with the existing measurements. Section IV compares the performance of multi-polarized MIMO systems with the traditional uni-polarized MIMO systems. We conclude this work with some remarks in Section V.

## II. ANALYSIS OF CORRELATION BETWEEN ANTENNAS

The correlation between antennas (both for transmitting antennas and receiving antennas) is a very important parameter in MIMO communication systems. It is significant to decrease the correlation between antennas to increase the MIMO systems capacity by using multi-polarized antennas. In this section, we analyze the correlation between multi-polarized antennas, and the correlation is influenced by many parameters such as XPI, XPD, antenna tilt and etc.

### A. CORRELATED TRANSMISSION SCENARIO

A 3-D uni-polarized MIMO systems transmission scenario of two antennas is shown in Fig. 1(a). The $x$-$S_1$-$y$ plane is the horizontal plane. Usually, we regard the ground as a reference, which means the antennas perpendicular to the ground are vertically polarized antennas, and the antennas parallel to the ground are horizontally polarized antennas. The two

**TABLE 1. Comparison of mean AS under different communication environments [21].**

| Frequency (MHz) | Urban | Suburban | Countryside | Indoor |
|---|---|---|---|---|
| 1000 | | | | $20^\circ \sim 60^\circ$ |
| 1800 | $8^\circ$ | $5^\circ$ | | |
| 1845 | | | $<10^\circ$ | |
| 1873 | $3^\circ \sim 15^\circ$ | | | |
| 2100 | $7^\circ \sim 12^\circ$ | $3^\circ \sim 18^\circ$ | | |
| 2154 | | | $10.3^\circ$ | |
| 2200 | | | $3^\circ$ | |
| 7000 | | | | $22^\circ \sim 26^\circ$ |

antennas Rx1 and Rx2 are perpendicular to the $x$-$S_1$-$y$ plane, thus they are vertically polarized antennas. The two antennas are in the far-field of the signals, therefore, the directions of the incident waves at the two antennas are parallel and they only have a transmission distance difference $SS_1$. This is a typical traditional uni-polarized MIMO systems. The multipath signals come from arbitrary directions with the AAoAs $\alpha_n$ ($n \in \{1, 2 \ldots N\}$) and EAoAs $\beta_n$ ($n \in \{1, 2 \ldots N\}$) for both antennas. The antenna spacing $S_1S_2$ is d, and $S_1S_0$ is the projection of $S_1S$ on the $x$-$S_1$-$y$ plane. $\angle SS_1S_0$ is the EAoAs $\beta_n$, and $\angle yS_1S_0$ is the AAoAs $\alpha_n$, then the angle $\angle S_0\, S_1\, S_2$ equals to $(\pi/2 - \alpha_n)$. Therefore, the angle $\angle SS_1\, S_2$ is given by

$$\begin{aligned} cos\angle SS_1S_2 &= cos\angle S_0S_1S_2 cos\angle SS_1S_0 \\ &= cos(\pi/2 - \alpha_n)cos(\beta_n). \end{aligned} \tag{1}$$

The transmission distance difference of the antennas is $SS_1$, and the corresponding time delay difference is $SS_1$/c=d$cos(\pi/2 - \alpha_n)cos(\beta_n)$/c. Regarding antenna Rx2 as a reference antenna, the channel impulse responses at two antennas can be expressed as

$$h_1 = \sum_{n=1}^{N} A_n e^{j(\phi_n + 2\pi d cos(\frac{\pi}{2} - \alpha_n)cos(\beta_n)/\lambda)} \tag{2}$$

$$h_2 = \sum_{n=1}^{N} A_n e^{j\phi_n} \tag{3}$$

where $A_n$ is the $n$th path receiving amplitude and $\phi_n$ is the $n$th path receiving phase. The total number of the multipath is $N$. $\lambda$ is the carrier wavelength. Therefore, the correlation between antenna Rx1 and Rx2 is given by

$$\begin{aligned} \rho_{12} &= E\{h_1 {h_2}^*\} \\ &= E\{\sum_{n=1}^{N} A_n^2 e^{j2\pi d cos(\frac{\pi}{2} - \alpha_n)cos(\beta_n)/\lambda}\}. \end{aligned} \tag{4}$$

As $N \to \infty$, the discrete AAoAs $\alpha_n$ and discrete EAoAs $\beta_n$ can be replaced with continuous random variables $\alpha$ and $\beta$ having joint probability density function (pdf) $p(\alpha, \beta)$ [8]. It is assumed that AAoAs and EAoAs are independent of each other, then we have $p(\alpha, \beta) = p(\alpha)p(\beta)$. The discrete amplitude $A_n$ can be also replaced with receiving amplitude variable $A$. (4) can be written as

$$\rho_{12} = A^2 \int\int e^{j2\pi d cos(\frac{\pi}{2} - \alpha)cos(\beta)/\lambda} p(\alpha)p(\beta)d\beta d\alpha. \tag{5}$$

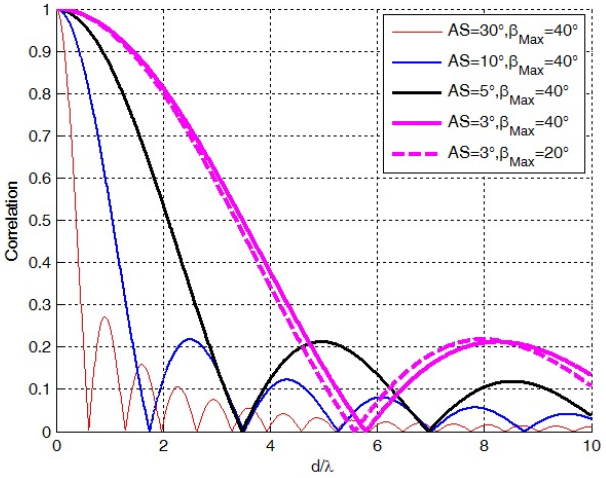


**FIGURE 2. Correlation between uni-polarized MIMO antennas versus antenna spacing.**

Both AAoAs and EAoAs distributions are determined by the communication environment (e.g., indoor or outdoor, urban or suburban, macrocell or microcell). There are many different distributions to characterize the AAoAs and EAoAs distributions, such as uniform, Gaussian, Laplacian. Usually, we use the uniform distribution with certain angle spread (AS) to characterize the AAoAs distribution, which is defined as

$$p(\alpha) = \frac{1}{2\Delta\alpha}, \quad -\Delta\alpha + \alpha_0 \le \alpha \le \Delta\alpha + \alpha_0 \tag{6}$$

where $\alpha_0$ is the mean AAoAs, $\Delta\alpha = \sqrt{3}\sigma_A$ [20], and $\sigma_A$ is the AS. Table 1 has summarized the mean AS under different communication environments [21]. For the EAoAs distributions, we use the cosine pdf [22]

$$p(\beta) = \frac{\pi}{4\beta_{max}} \cos(\frac{\pi}{2}\frac{\beta}{\beta_{max}}), \quad |\beta| \le \beta_{max} \le \frac{\pi}{2} \tag{7}$$

where $\beta_{max}$ lies in the range $20^\circ < \beta_{max} < 45^\circ$.

We can obtain the correlation between antennas by substituting (6), (7) to (5), and the correlation curves are shown in Fig. 2. The amplitude is normalized and the mean AAoAs

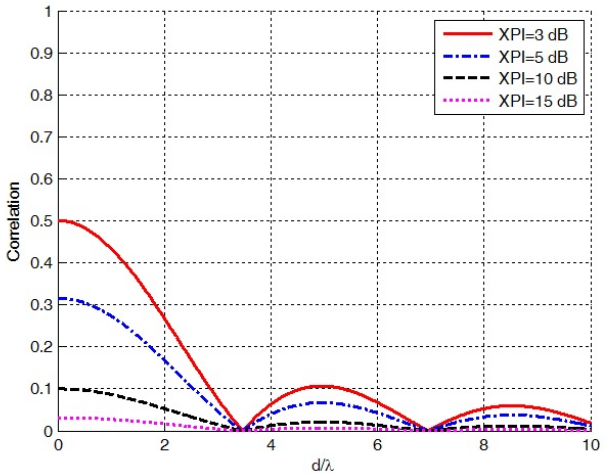


**FIGURE 3.** Correlation between multi-polarized MIMO antennas at different XPI.

is set to be 0°. From Fig. 2 we can see that the correlation is sensitive to the AAoAs distribution while the EAoAs distribution has a slight effect on the correlation, and the larger AS results in a lower correlation. The AS dimension depends on the scattering of the communication environment, which means the richer scattering makes the AS larger at the receiver, and the small AS represents the insufficient scattering. Hence, the traditional uni-polarized MIMO systems need a rich scattering or large antenna spacing to decrease the correlation to achieve significant MIMO gain.

### B. CORRELATION ANALYSIS OF MULTI-POLARIZED MIMO ANTENNAS

A 3-D multi-polarized MIMO systems transmission scenario of two antennas is shown in Fig. 1(b). The transmission scenario in Fig. 1(b) is the same as Fig. 1(a), and the only difference is the antenna Rx2. Rx2 parallels to the horizontal plane, therefore, Rx2 is a horizontally polarized antenna. They compose dual-polarized (or cross-polarized) antennas, which is a typical multi-polarized MIMO system. Theoretically, the correlation between two cross-polarized antennas should be 0, but such is not the case in practice due to three main mechanisms [23]. The first is that the antenna has a finite XPI, which means the antenna can more or less receive the cross-polarization component as well. The second is the tilt of antennas, which can take place at both ends of the link. Finally, the most important mechanism is the channel depolarization, and it can be described by the channel XPD. Hence, we take all the three mechanisms into account to analyze the correlation between multi-polarized antennas.

Usually, an antenna is designed to receive a signal having a certain polarization, and it is completely isolated to the cross-polarization component (i.e., the vertically polarized antennas have zero gain to the horizontally polarized direction signal and vice versa) [6]. But the antennas can more or less receive the cross-polarization component on the basis of the antenna theory. A commonly used method for describing this antenna performance is to define the cross-polar isolation (XPI), which is the ratio of the co-polarization receive gain to the cross-polarization receive gain

$$XPI = \frac{G_{VV}}{G_{VH}} = \frac{G_{HH}}{G_{HV}} \tag{8}$$

where $G_{VV}$ and $G_{HH}$ are co-polarization receive gain, which should be 1 for both antennas, and $G_{VH}$ and $G_{HV}$ are cross-polarization receive gain. We assume that the antenna receive gain is identical to every multipath. The antenna XPI is influenced by the antenna design regardless of the communication environment, and it is the performance of the antenna itself. Then the channel impulse responses at two multi-polarized antennas including antenna XPI can be expressed as

$$h_{V1}^{XPI} = \sum_{n=1}^{N}(G_{VV}A_{V,n} + G_{VH}A_{H,n}) \times e^{j(\phi_n + 2\pi d cos(\frac{\pi}{2}-\alpha_n)cos(\beta_n)/\lambda)} \tag{9}$$

$$h_{H2}^{XPI} = \sum_{n=1}^{N}(G_{HH}A_{H,n} + G_{HV}A_{V,n})e^{j\phi_n} \tag{10}$$

where $A_{V,n}$ is the $n$th path vertically polarized receiving amplitude and $A_{H,n}$ is the $n$th path horizontally polarized receiving amplitude. For Rx1(V), it can receive the vertically polarized signals and more or less can receive the horizontally polarized signals due to the finite XPI. Therefore, the $n$th path receiving amplitude for Rx1(V) is $(G_{VV}A_{V,n}+G_{VH}A_{H,n})$, and the $n$th path receiving amplitude for Rx2(H) is $(G_{HH}A_{H,n} + G_{HV}A_{V,n})$. Therefore, the correlation between Rx1(V) and Rx2(H) is expressed as

$$\begin{aligned}\rho_{VH}^{XPI} &= E\{h_{V1}^{XPI*}h_{H2}^{XPI}\} \\ &= (G_{VV}A_V + G_{VH}A_H)(G_{HH}A_H + G_{HV}A_V) \\ &\quad \times \int\int e^{j2\pi d cos(\frac{\pi}{2}-\alpha)cos(\beta)/\lambda}p(\alpha)p(\beta)d\beta d\alpha\end{aligned} \tag{11}$$

where $A_V$ is the vertically polarized receiving amplitude and $A_H$ is the horizontally polarized receiving amplitude.

Fig. 3 shows the correlation curves at different XPI values. The AS is set to be a typical value 5°, $\beta_{max} = 40°$ and the arriving signals are assumed to be vertically polarized. XPI indicates the ability to isolate the cross-polarized signal of antennas, and the higher XPI means less cross-polarized receive power. Therefore, the correlation declines as the XPI increases because of the improvement of isolation ability. When XPI = 0 dB, the antennas can receive all the cross-polarized signal and it reduces to the traditional uni-polarized MIMO systems. When XPI goes to infinite, the correlation will be 0 because of the complete isolation of the cross-polarized signal, and they become two completely uncorrelated antennas. We can see that the multi-polarized antennas obtain a low correlation at the cost of power loss.

In real wireless communication channels, the reflections, diffractions, and scattering of signals in the wireless channel may result in channel depolarization, and the polarization orientation may change after passing through the wireless

channel. A commonly used method for describing channel depolarization is to define the cross-polarization discrimination (XPD) [24]

$$XPD_V = \frac{\mathrm{E}\{|h_{VV}|^2\}}{\mathrm{E}\{|h_{HV}|^2\}} = \frac{1-a_V}{a_V}, \quad a_V = \frac{1}{XPD_V+1} \tag{12}$$

$$XPD_H = \frac{\mathrm{E}\{|h_{HH}|^2\}}{\mathrm{E}\{|h_{VH}|^2\}} = \frac{1-a_H}{a_H}, \quad a_H = \frac{1}{XPD_H+1} \tag{13}$$

where $h_{XY}(X, Y \in V, H)$ is the component in the $XY$ channel, and E{} represents the expectation operator. $a_X (0 < a_X \leq 1)$ is defined for the convenience of modeling and computing, which is directly related to the $XPD_X$ for the channel and corresponds to the part of the radiated power that is coupled from $V$ to $H$ and vice versa [6]. When there is no leakage from the $X$ polarized component to the $Y$ polarized component, $a_X$ is equal to 0, otherwise, there is leakage between the polarizations when $0 < a_X \leq 1$. Jian *et al.* [24] pointed out that the received power in the vertical-to-vertical channel is normally higher than that in the horizontal-to-horizontal channel, and polarization selectivity favors vertical polarization, which means $\mathrm{E}\{|h_{VV}|^2\} > \mathrm{E}\{|h_{HH}|^2\}$. Another parameter is the co-polar ratio (CPR) to describe the imbalance between vertical-to-vertical channel and horizontal-to-horizontal channel, which is defined as

$$CPR = \frac{\mathrm{E}\{|h_{VV}|^2\}}{\mathrm{E}\{|h_{HH}|^2\}} = \frac{1-a_V}{1-a_H}. \tag{14}$$

Then the channel impulse responses at two antennas including antenna XPI and channel XPD can be expressed as

$$\begin{aligned} h_{V1}^{XPI,XPD} = &\sum_{n=1}^{N}(G_{VV}[A_{V,n}(1-a_V)+A_{H,n}a_H] \\ &+ G_{VH}[A_{H,n}(1-a_H)+A_{V,n}a_V]) \\ &\times e^{j(\phi_n+2\pi d\cos(\frac{\pi}{2}-\alpha_n)\cos(\beta_n)/\lambda)} \end{aligned} \tag{15}$$

$$\begin{aligned} h_{H2}^{XPI,XPD} = &\sum_{n=1}^{N}(G_{HH}[A_{H,n}(1-a_H)+A_{V,n}a_V] \\ &+ G_{HV}[A_{V,n}(1-a_V)+A_{H,n}a_H]) \times e^{j\phi_n}. \end{aligned} \tag{16}$$

$A_{X,n}(1-a_X)$ is the $n$th path signal maintain in the co-polarization and $A_{X,n}a_X$ is the $n$th path signal leakage to the cross-polarization at the antennas [25]. Then the correlation between Rx1(V) and Rx2(H) is expressed as

$$\begin{aligned} \rho_{VH}^{XPI,XPD} &= E\{h_{V1}^{XPI,XPD*}h_{H2}^{XPI,XPD}\} \\ &= (G_{VV}[A_V(1-a_V)+A_Ha_H] \\ &\quad + G_{VH}[A_H(1-a_H)+A_Va_V]) \\ &\quad \times (G_{HH}[A_H(1-a_H)+A_Va_V] \\ &\quad + G_{HV}[A_V(1-a_V)+A_Ha_H]) \\ &\quad \times \int\int e^{j2\pi d\cos(\frac{\pi}{2}-\alpha)\cos(\beta)/\lambda}p(\alpha)p(\beta)d\beta d\alpha. \end{aligned} \tag{17}$$

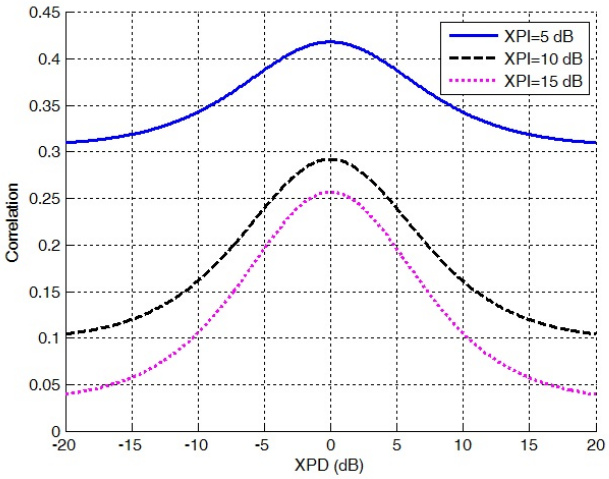


**FIGURE 4.** Correlation between multi-polarized MIMO antennas vs. XPD.

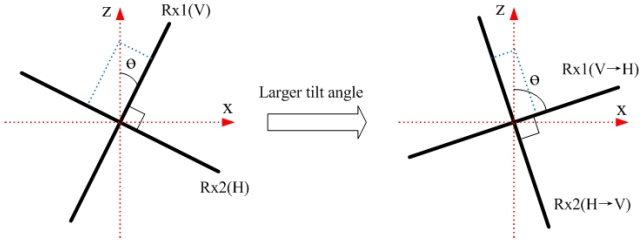


**FIGURE 5.** Antenna tilt.

Fig. 4 shows the correlation between multi-polarized MIMO antennas vs. XPD (CPR=0 *dB*), and the antenna spacing equals to $\lambda/2$. The correlation reaches the maximum value when XPD=0 *dB*. This is because half of the signals leakage to the cross-polarization when XPD=0 *dB*, and this makes the strongest correlation between two cross-polarized antennas. As the XPD increases or decreases, the correlation declines because more signals will maintain in the co-polarized channel or leakage to the cross-polarized channel to weaken the correlation. Unlike the XPI, XPD is used to describe the wireless channels and is determined by the communication environment regardless of the antennas.

The antenna tilt is another factor that can influence the correlation and power imbalance. In fixed-to-mobile communications systems, the antenna tilt takes place in the mobile terminals, and in mobile-to-mobile communication systems, it happens in both transmitting and receiving terminals. Fig. 5 shows the transmission scenario with antenna tilt, and here we use the co-located cross-polarized antennas. There is an angle of tilt $\theta$ ($0° \leq \theta \leq 90°$) between the Rx1(V) and the vertical direction. As $\theta$ increases, the vertically polarized antenna becomes the horizontally polarized antenna, and the horizontally polarized antenna becomes the vertically polarized antenna. When $\theta = 90°$, they are completely exchanged. Hence, it is a symmetrical process and the receiving amplitude can be decomposed to the two cross-polarized antennas.

The channel impulse responses can be expressed as

$$\begin{aligned} h_{V1}^{XPI,XPD,Tilt} &= \sum_{n=1}^{N}(G_{VV}\{[A_{V,n}(1-a_V)+A_{H,n}a_H]cos(\theta) \\ &+ [A_{H,n}(1-a_H)+A_{V,n}a_V]sin(\theta)\} \\ &+ G_{VH}\{[A_{H,n}(1-a_H)+A_{V,n}a_V]cos(\theta) \\ &+ [A_{V,n}(1-a_V)+A_{H,n}a_H]sin(\theta)\}) \\ &\times e^{j(\phi_n+2\pi dcos(\alpha_n)cos(\beta_n)/\lambda)} \end{aligned} \tag{18}$$

$$\begin{aligned} h_{H1}^{XPI,XPD,Tilt} &= \sum_{n=1}^{N}(G_{HH}\{[A_{H,n}(1-a_H)+A_{V,n}a_V]cos(\theta) \\ &+ [A_{V,n}(1-a_V)+A_{H,n}a_H]sin(\theta)\} \\ &+ G_{HV}\{[A_{V,n}(1-a_V)+A_{H,n}a_H]cos(\theta) \\ &+ [A_{H,n}(1-a_H)+A_{V,n}a_V]sin(\theta)\}) \times e^{j\phi_n}. \end{aligned} \tag{19}$$

The correlation between Rx1(V) and Rx2(H) including XPI,XPD and antennas tilt can be expressed as

$$\begin{aligned} \rho_{VH}^{XPI,XPD,Tilt} &= E\{h_{V1}^{XPI,XPD,Tilt*}h_{H2}^{XPI,XPD,Tilt}\} \\ &= (G_{VV}\{[A_V(1-a_V)+A_Ha_H]cos(\theta) \\ &+ [A_H(1-a_H)+A_Va_V]sin(\theta)\} \\ &+ G_{VH}\{[A_H(1-a_H)+A_Va_V]cos(\theta) \\ &+ [A_V(1-a_V)+A_Ha_H]sin(\theta)\}) \\ &\times (G_{HH}\{[A_H(1-a_H)+A_Va_V]cos(\theta) \\ &+ [A_V(1-a_V)+A_Ha_H]sin(\theta)\} \\ &+ G_{HV}\{[A_V(1-a_V)+A_Ha_H]cos(\theta) \\ &+ [A_H(1-a_H)+A_Va_V]sin(\theta)\}) \\ &\times \int\int e^{j2\pi dcos(\frac{\pi}{2}-\alpha)cos(\beta)/\lambda}p(\alpha)p(\beta)d\beta d\alpha. \end{aligned} \tag{22}$$

Fig. 6 shows the correlation between multi-polarized MIMO antennas vs. $\theta$. Also, the antenna spacing is set to be $\lambda/2$ and XPI equals to 10 dB. The correlation reaches the maximum value when $\theta = 45°$ at different XPD values, and the correlation is symmetrical about $\theta = 45°$ because the antenna tilt process is symmetrical about 45°.

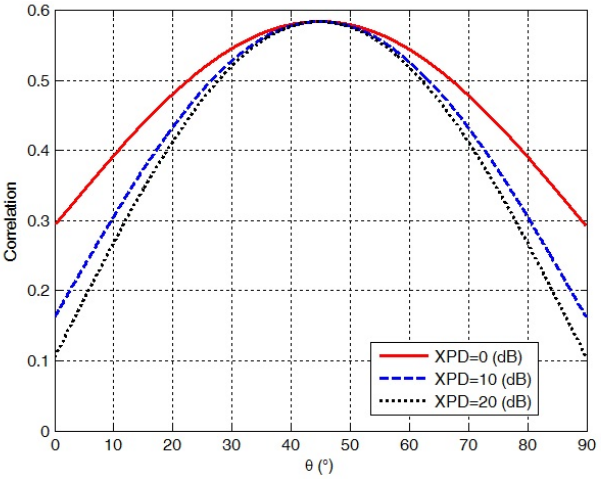


**FIGURE 6.** Correlation between multi-polarized MIMO antennas vs. $\theta$.

## III. CHANNEL MODELING AND VALIDATION FOR MULTI-POLARIZED MIMO SYSTEMS

In this section, we model the multi-polarized MIMO systems channel as a Ricean fading channel including XPI, XPD and antenna tilt. Then we compare our model with the existing measurements for validation, and it shows the proposed model is well in agreement with the measurements.

### A. CHANNEL MODELING

Multi-polarized MIMO systems channel can be modeled as a Ricean fading channel, which means the channel matrix is composed of a fixed (LoS) part and a random or scattering (NLoS) part according to [12]

$$\mathbf{H} = \sqrt{\frac{K}{K+1}}\bar{\mathbf{H}} + \sqrt{\frac{1}{K+1}}\tilde{\mathbf{H}} \tag{23}$$

where $K$ is the Ricean $K$-factor, and it is defined as the power ratio of the LoS component to the NLoS component. $\bar{\mathbf{H}}$ is a deterministic matrix representing the LoS part while $\tilde{\mathbf{H}}$ is a random matrix representing the NLoS part. When $K \to \infty$, only the LoS component is considered, and the channel matrix is determined by the LoS component. When $K = 0$, there is only a scattering component and it becomes a Rayleigh fading channel [6]. Otherwise, the Ricean fading channel has both LoS and NLOS scattering components, which can well describe the transmission channel in reality.

$$\begin{aligned} \tilde{\mathbf{H}} = \Bigg\{ &\begin{bmatrix} G_{VV} & G_{VV} \\ G_{HH} & G_{HH} \end{bmatrix} \odot \left( \begin{bmatrix} cos(\theta) & sin(\theta) \\ sin(\theta) & cos(\theta) \end{bmatrix} \begin{bmatrix} 1-\alpha_V & \alpha_H \\ \alpha_V & 1-\alpha_H \end{bmatrix} \right) \\ &+ \begin{bmatrix} G_{VH} & G_{VH} \\ G_{HV} & G_{HV} \end{bmatrix} \odot \left( \begin{bmatrix} cos(\theta) & sin(\theta) \\ sin(\theta) & cos(\theta) \end{bmatrix} \begin{bmatrix} \alpha_V & 1-\alpha_H \\ 1-\alpha_V & \alpha_H \end{bmatrix} \right) \Bigg\} \\ &\odot \left( \begin{bmatrix} 1 & \rho_r \\ \rho_r^* & 1 \end{bmatrix} \mathbf{H}_{\mathbf{i.i.d.}} \begin{bmatrix} 1 & \rho_t \\ \rho_t^* & 1 \end{bmatrix} \right) \end{aligned} \tag{20}$$

$$\bar{\mathbf{H}} = \begin{bmatrix} G_{VV} & G_{VH} \\ G_{HV} & G_{HH} \end{bmatrix} \begin{bmatrix} cos(\theta) & sin(\theta) \\ sin(\theta) & cos(\theta) \end{bmatrix} \odot \bar{\mathbf{H}}_d \tag{21}$$

In addition, the correlated channel model can be modeled as Kronecker model [21]

$$\tilde{\mathbf{H}}_c = (\mathbf{R_r}^{1/2}\mathbf{H_{i.i.d.}}\mathbf{R_t}^{1/2})$$
$$\mathbf{R_r} = \begin{bmatrix} 1 & \rho_r \\ \rho_r^* & 1 \end{bmatrix}, \quad \mathbf{R_t} = \begin{bmatrix} 1 & \rho_t \\ \rho_t^* & 1 \end{bmatrix} \tag{24}$$

where $\mathbf{H_{i.i.d.}}$ is a matrix of independent and identically distributed (i.i.d.) zero mean complex-valued Gaussian random variables to describe the uncorrelated channel with power balance. $\mathbf{R_r}$ and $\mathbf{R_t}$ are receiving and transmitting antennas correlation matrices. $\rho_r$ and $\rho_t$ are receiving and transmitting antennas correlation, which are obtained from (22). In addition, the power imbalance has to be considered in the multi-polarized MIMO systems. The power imbalance caused by the polarization mismatch (XPD, antenna tilt) and the finite XPI, and it can be described by polarization matrix

$$\tilde{\mathbf{H}}_p = \tilde{\mathbf{G}}_{||} \odot (\tilde{\mathbf{T}}\tilde{\mathbf{H}}_{||}) + \tilde{\mathbf{G}}_{|-} \odot (\tilde{\mathbf{T}}\tilde{\mathbf{H}}_{|-})$$
$$\tilde{\mathbf{G}}_{||} = \begin{bmatrix} G_{VV} & G_{VV} \\ G_{HH} & G_{HH} \end{bmatrix}, \quad \tilde{\mathbf{G}}_{|-} = \begin{bmatrix} G_{VH} & G_{VH} \\ G_{HV} & G_{HV} \end{bmatrix}$$
$$\tilde{\mathbf{H}}_{||} = \begin{bmatrix} 1-\alpha_V & \alpha_H \\ \alpha_V & 1-\alpha_H \end{bmatrix}, \quad \tilde{\mathbf{H}}_{|-} = \begin{bmatrix} \alpha_V & 1-\alpha_H \\ 1-\alpha_V & \alpha_H \end{bmatrix}$$
$$\tilde{\mathbf{T}} = \begin{bmatrix} cos(\theta) & sin(\theta) \\ sin(\theta) & cos(\theta) \end{bmatrix} \tag{25}$$

where $\tilde{\mathbf{G}}_{||}$ is the co-polarization receive gain matrix, and $\tilde{\mathbf{G}}_{|-}$ is the cross-polarization receive gain matrix. $\tilde{\mathbf{H}}_{||}$ is the co-polarization XPD matrix to describe the signals maintain in the co-polarized channel, and $\tilde{\mathbf{H}}_{|-}$ is the cross-polarization XPD matrix to describe the signals leakage to the cross-polarized channel. $\tilde{\mathbf{T}}$ is the antenna tilt matrix. Hence, the Rayleigh matrix (or channel) including correlation and power imbalance is

$$\tilde{\mathbf{H}} = \tilde{\mathbf{H}}_p \odot \tilde{\mathbf{H}}_c \tag{26}$$

and it is shown in (20), as shown at the bottom of the previous page, where $\odot$ is the corresponding elements multiplication. Then the fixed (deterministic) matrix is shown in (21), as shown at the bottom of the previous page, where the elements of $\bar{\mathbf{H}}_d$ have unit power.

### B. VALIDATION OF THE MODEL

The whole channel can be obtained by substituting (20) (21) to (23), and the generalized MIMO systems capacity formula is expressed as [26]

$$\mathbf{C} = \log_2[\det(\mathbf{I} + \frac{\gamma}{\mathrm{N_t}}\mathbf{H}\mathbf{H}^{\mathbf{T}})]\text{bps/Hz} \tag{27}$$

where $\mathbf{I}$ is the identity matrix, and $\mathbf{H}$ denotes the channel matrix, $\mathbf{H}^{\mathbf{T}}$ is its conjugate transpose. $\gamma$ is the average receive signal-to-noise ratio (SNR), and $N_t$ is the number of the transmitting antennas.

Soma *et al.* presented outdoor $2 \times 2$ MIMO fixed wireless propagation measurements at 2.48 GHz conducted in the suburban residential areas of San Jose, California [27]. The measurements included path loss, Ricean K-factor, XPD and

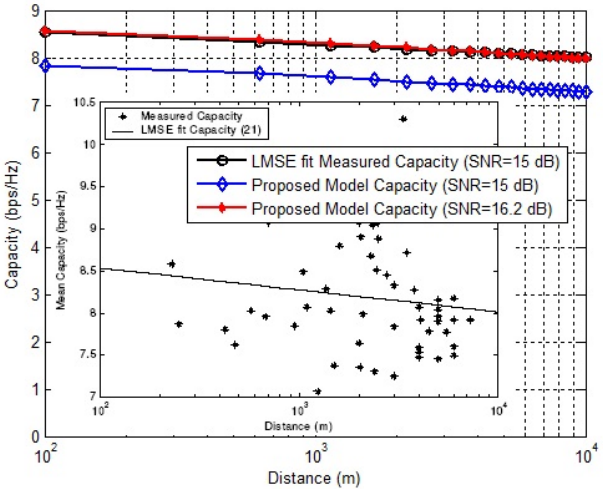


**FIGURE 7.** Comparison of multi-polarized MIMO systems capacity and measurements at 2.48 GHz.

capacity. Both the transmitting antennas and the receiving antennas are dual-polarized antennas, and we compare our model with the measurements for validation. All the measurements in [27] are expressed as a set of equations by fitting the measured data with least mean square error (LMSE) regression curves and given by

$$K_m = 5.53 - 2.93log_{10}(D/D_0) \tag{28}$$
$$XPD_m = 3.7 - 2.93log_{10}(D/D_0) \tag{29}$$
$$C_m = 8.27 - 0.26log_{10}(D/D_0) \tag{30}$$

where $D$ is the distance between transmitting antennas and receiving antenna, and $D_0$ corresponds to a reference distance in the far-field of the antenna, which is typically set to be 1 km. We substitute the XPD and K-value with the measurements $XPD_m$ and $K_m$ in our model, then we can obtain the correlation and capacity as a function of the distance between transmitting antennas and receiving antennas $D$, and we compare the capacity of our model with the measured capacity $C_m$.

We set the simulation parameters according to the measurement environment in [27] strictly. The two transmitting antennas were separated by 10 wavelengths and at the receiver side, two co-located receiving antennas were used. Therefore, the antenna spacing is set to be $10\lambda$ at the transmitter and 0 at the receiver. The XPI and antenna tilt were not considered in [27], hence, $\theta$ equals to $0^\circ$ and XPI is set to be a typical value 10 dB. Since the measurements were conducted in outdoor suburban residential areas, the AS is chosen to be a mean value $10^\circ$ according to the table 1. The SNR is a fixed value of 15 dB in the measurements, and we set the SNR to be 15 dB in the simulation. Fig. 7 shows the comparison of the capacity in our model with the measurements. The simulations and measurements are well in agreement and the simulations have slightly lower capacity, which is most likely due to the pessimistic complex envelope correlation [19]. And the measurements in [27] have considered the path loss, which we did not take into account in our model. Hence,

**TABLE 2. Comparison between the multi-polarized MIMO systems and uni-polarized MIMO systems in different communication scenarios.**

| | Low SNR | High SNR | Low XPD | High XPD | Compact structure | Antenna tilt | Robustness |
|---|---|---|---|---|---|---|---|
| Uni-polarized MIMO systems | √ | | | √ | | | Bad |
| Multi-polarized MIMO systems | | √ | √ | √ | √ | √ | Good |

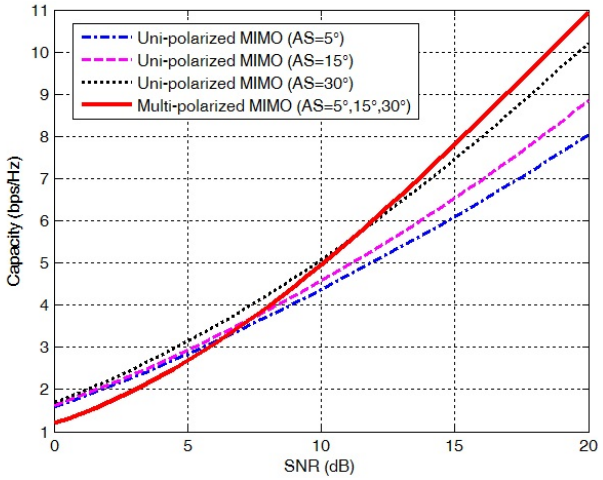


**FIGURE 8. Comparison of capacity between multi-polarized MIMO systems and uni-polarized MIMO systems (d=λ/2, XPI=10 dB, XPD=10 dB, $\theta$=0°, K=8 dB).**

we improve our SNR a little to 16.2 dB, and from Fig. 7 we can see that the proposed model capacity perfectly matches the measurements when SNR=16.2 dB.

## IV. COMPARISON AND ANALYSIS

According to the reported measurements in [27], Ricean K-factor can be equaled to a mean value 8 dB and $\theta$=0° when considering other parameters. d=λ/2 and XPI is a typical value 10 dB. XPD is set to be 10 dB to observe the effect of other parameters on the systems performance. SNR is 15 dB and AS is set according to table 1. When considering one parameter of all, the other parameters are fixed. The number of antennas at both ends for two cases is two (2×2 MIMO). For uni-polarized MIMO systems, they are vertically polarized antennas, and for the proposed multi-polarized MIMO systems, they are cross-polarized antennas structure. Fig. 8 is the comparison of capacity between multi-polarized MIMO systems and uni-polarized MIMO systems, and from which we can see that the uni-polarized MIMO systems capacity is sensitive to the AS while the performance of multi-polarized MIMO systems is unaffected by AS. For uni-polarized MIMO systems, the larger AS makes the lower correlation between antennas, hence resulting in a higher capacity. Therefore, the uni-polarized MIMO systems need rich scattering in the communication environment to reduce the correlation and obtain the high capacity. The AS almost has no effect on the multi-polarized MIMO systems because the correlation between multi-polarized antennas is already extremely low, and the AS has no influence on it (actually, there are also three curves of multi-polarized MIMO systems with different AS, but they are overlapped). For a multi-polarized MIMO system, it does not need rich scattering because the correlation is already low, and its performance is robust to the communication environment. Although the multi-polarized MIMO system has low correlation, it also has the power loss because of the polarization mismatch. Fig. 8 shows the multi-polarized MIMO systems do not always outperform uni-polarized MIMO systems. In the high SNR region, the multi-polarized MIMO systems are more effective because of the reduction in the correlation between antennas. While in the low SNR region, the reduction in the correlation of the multi-polarized MIMO systems is not enough to compensate for the power loss in the co-polarized component [7]. Hence, the multi-polarized MIMO systems have lower capacity when SNR is low.

AS is set to be a small value of 5° to make the correlation strong to show the effect of antenna spacing and XPI on the systems performance in Fig. 9 (a) and (b). The uni-polarized MIMO systems capacity increases as the antenna spacing increases as shown in Fig. 9 (a), because the correlation decreases as the antenna spacing increases. In comparison, the multi-polarized MIMO systems capacity has a slight change, because the antenna spacing has a slight effect on the correlation between multi-polarized antennas and the correlation is already very low even when the two antennas are co-located. Therefore, the multi-polarized antennas can realize compact structure and the space efficiency especially in the user terminals. Fig. 9 (b) shows how the capacity is influenced by the XPI. When the XPI=0 dB, the antennas can receive all the cross-polarized power, and the multi-polarized MIMO systems reduce to the uni-polarized MIMO systems. The multi-polarized MIMO systems capacity increases as the XPI increases because the correlation decreases as the XPI increases, therefore, it is significant to improve the XPI during the antenna's design.

Ricean K-factor is set to be 0 dB to enhance the scattering component to show the effect of XPD on the systems performance in Fig. 9 (c), and AS is set to be a big value 20° to weaken the correlation effect to show the effect of XPD and antenna tilt on the systems performance in Fig. 9 (c) and (d). Fig. 9(c) shows the capacity changes as the XPD varies. From which we can see the capacity of uni-polarized MIMO systems decreases drastically as the XPD decreases. This is because the uni-polarized MIMO systems will lose most of the power due to the polarization mismatch at low XPD. And multi-polarized MIMO systems always have

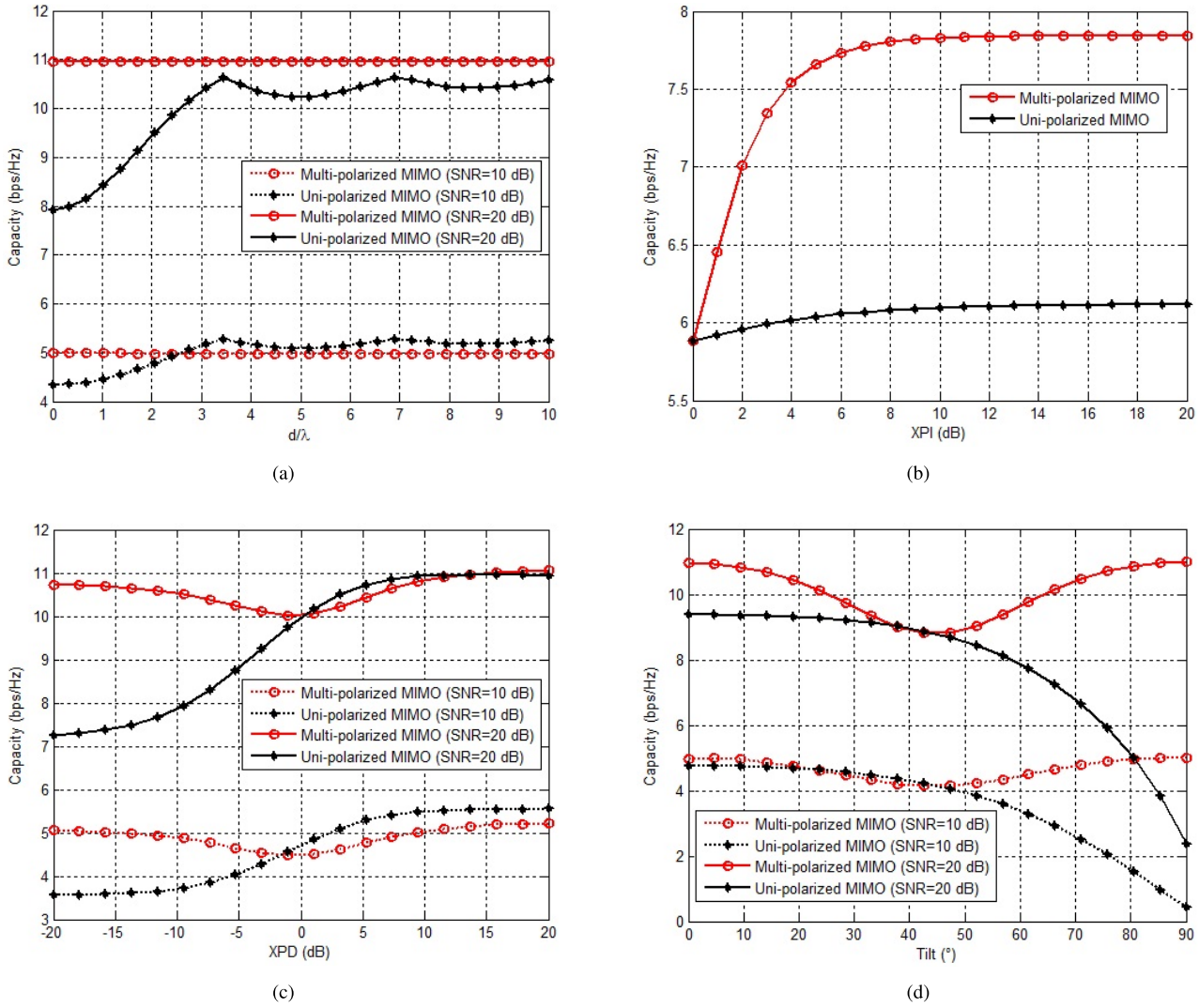


**FIGURE 9.** (a) Capacity of multi-polarized MIMO systems and uni-polarized MIMO systems vs. antenna spacing (XPI=10 dB, XPD=10 dB, $\theta$=0°, K=8 dB, AS=5°). (b) Capacity of multi-polarized MIMO systems and uni-polarized MIMO systems vs. XPI (SNR=15 dB, d=$\lambda$/2, XPD=10 dB, $\theta$=0°, K=8 dB, AS=5°). (c) Capacity of multi-polarized MIMO systems and uni-polarized MIMO systems vs. XPD (d=$\lambda$/2, XPI=10 dB, $\theta$=0°, K=0 dB, AS=20°). (d) Capacity of multi-polarized MIMO systems and uni-polarized MIMO systems vs. antenna tilt (d=$\lambda$/2, XPI=10 dB, XPD=10 dB, K=8 dB, AS=20°).

cross-polarized antenna to receive the cross-polarized signal, therefore, the XPD has a slight effect on the multi-polarized MIMO systems and it achieves better performance in such situations. We change the antenna tilt at one end in Fig. 9 (d), and the capacity is symmetrical about tilt angle equals to 45° because the antenna tilt process is symmetrical about 45° for the multi-polarized MIMO systems. While the capacity of uni-polarized MIMO systems decreases drastically as the tilt increases because the uni-polarized MIMO systems will lose most of the power due to the polarization mismatch when the antenna tilt angle is large. The worst case for uni-polarized MIMO systems is when the tilt angle becomes 90°, it becomes cross-polarization reception resulting in the most power loss scenario.

The multi-polarized antennas have been implemented in MIMO systems to reduce the antenna correlation and realize the space efficiency, but it also causes the power loss and imbalance between antennas. Therefore, the multi-polarized MIMO systems do not always outperform uni-polarized MIMO systems. Table 2 summarizes the comparison between the multi-polarized MIMO systems and uni-polarized MIMO systems in different communication scenarios. $\surd$ means we can choose this kind of MIMO systems in this communication scenario. The performance of multi-polarized MIMO systems have robustness to the communication scenarios including antenna spacing, scattering condition, XPD and antenna tilt. But if the SNR is low, the multi-polarized MIMO systems can not be used because of the severe power loss. Finally, if the space efficiency and the miniaturization of equipments are of primary concern, the multi-polarized antennas would be the best choice.

## V. CONCLUSION

In this paper, a geometrical model for multi-polarized MIMO systems including antenna XPI, channel XPD, antenna tilt parameters is proposed. The correlation between multi-polarized antennas is analyzed. Multi-polarized MIMO systems obtain a low correlation at the cost of power loss, and it is found that the correlation is not sensitive to the scattering condition. The multi-polarized MIMO systems is modeled as a Ricean fading channel, and it is shown that the XPI, XPD and antenna tilt have effect on the correlation and capacity simultaneously. The comparison between the proposed model and the existing measurements shows that the proposed model is well in agreement with the measurements. The comparison between the multi-polarized MIMO systems with the traditional uni-polarized MIMO systems shows that the performance of multi-polarized MIMO systems have robustness to the communication environment and the multi-polarized MIMO systems outperform the uni-polarized MIMO systems in many communication scenarios. Finally, as the number of antennas in MIMO systems increases to a large number in massive MIMO systems in the future 5th generation (5G) cellular networks, the multi-polarized antennas would be the best choice to realize the space efficiency and the miniaturization of equipments.

## REFERENCES

[1] C. Oestges, M. Guillaud, and M. Debbah, "Multi-polarized MIMO communications channel model, mutual information and array optimization," in *Proc. Wireless Commun. Netw. Conf. (WCNC)*, Mar. 2007, pp. 1057–1061.

[2] V. Erceg, D. Baum, S. Pitchaiah, and A. J. Paulraj, "Capacity obtained from multiple-input multiple-output channel measurements in fixed wireless environments at 2.5 GHz," in *Proc. IEEE Int. Conf. Commun. (ICC)*, May 2002, pp. 396–400.

[3] F. Quitin, C. Oestges, F. Horlin, and P. D. Doncker, "Multipolarized MIMO channel characteristics: Analytical study and experimental results," *IEEE Trans. Antennas Propag.*, vol. 57, no. 9, pp. 2739–2745, Sep. 2009.

[4] F. Quitin, C. Oestges, F. Horlin, and P. De Doncker, "Polarization measurements and modeling in indoor NLOS environments," *IEEE Trans. Wireless Commun.*, vol. 9, no. 1, pp. 21–25, Jan. 2010.

[5] X. Yin, Y. He, C. Ling, L. Tian, and X. Cheng, "Empirical stochastic modeling of multipath polarizations in indoor propagation scenarios," *IEEE Trans. Antennas Propag.*, vol. 63, no. 12, pp. 5799–5811, Dec. 2015.

[6] Y. He, X. Cheng, and G. L. Stuber, "On polarization channel modeling," *IEEE Wireless Commun.*, vol. 23, no. 1, pp. 80–86, Feb. 2016.

[7] M. T. Dao, V. A. Nguyen, Y. T. Im, S. O. Park, and G. Yoon, "3D polarized channel modeling and performance comparison of MIMO antenna configurations with different polarizations," *IEEE Trans. Antennas Propag.*, vol. 59, no. 7, pp. 2672–2682, Jul. 2011.

[8] S. Kwon and G. L. Stuber, "Geometrical theory of channel depolarization," *IEEE Trans. Veh. Technol.*, vol. 60, no. 8, pp. 3542–3556, Oct. 2011.

[9] X. Wu, C. Guo, C. Feng, and L. Lin, "Theoretical polarized channel model and analysis of XPD and polarization correlation under narrowband macrocell environment," in *Proc. 15th Wireless Pers. Multimedia Commun. (WPMC)*, Sep. 2012, pp. 468–472.

[10] J. Chen and T. Pratt, "Diversity measure of co-polarized and polarized MIMO architectures over wideband mobile-to-mobile channels," in *Proc. IEEE Military Commun. Conf. (MILCOM)*, Nov. 2013, pp. 1262–1267.

[11] C. Oestges, "Channel correlations and capacity metrics in MIMO dual-polarized Rayleigh and Ricean channels," in *Proc. IEEE Veh. Technol. Conf. (VTC-Fall)*, Sep. 2004, pp. 1453–1457.

[12] M. Coldrey, "Modeling and capacity of polarized MIMO channels," in *Proc. IEEE Veh. Technol. Conf. (VTC)*, May 2008, pp. 440–444.

[13] K. Jeon, B. Hui, K. Chang, H. Park, and Y. Park, "SISO polarized flat fading channel modeling for dual-polarized antenna systems," in *Proc. Int. Conf. Inf. Netw. (ICOIN)*, Feb. 2012, pp. 1–3.

[14] A. Ispas, X. Gong, C. Schneider, G. Ascheid, and R. Thoma, "Dual-polarized Ricean MIMO channels: Modeling and performance assessment," *IEEE Trans. Commun.*, vol. 61, no. 10, pp. 4218–4231, Oct. 2013.

[15] S. Jaeckel, K. Borner, L. Thiele, and V. Jungnickel, "A geometric polarization rotation model for the 3-D spatial channel model," *IEEE Trans. Antennas Propag.*, vol. 60, no. 12, pp. 5966–5977, Dec. 2012.

[16] C. A. Hofmann, D. Ogermann, and B. Lankl, "Measurement results for the comparison of multiple and single polarized MIMO channels in LOS, NLOS, indoor and outdoor scenarios," in *Proc. 17th Int. ITG Workshop Smart Antennas (WSA)*, Mar. 2013, pp. 1–8.

[17] A. Panahandeh, F. Quitin, J. M. Dricot, F. Horlin, C. Oestges, and P. De Doncker, "Orientation-free XPD and CPR model in outdoor-to-indoor and indoor-to-indoor channels," in *Proc. Antennas Propag. (EuCAP)*, Apr. 2010, pp. 1–5.

[18] A. Dunand and J. M. Conrat, "Polarization behaviour in urban macrocell environments at 2.2 GHz," in *Proc. 2nd Eur. Antennas Propag. (EuCAP)*, Nov. 2007, pp. 1–6.

[19] V. Erceg, P. Soma, D. S. Baum, and S. Catreux, "Multiple-input multiple-output fixed wireless radio channel measurements and modeling using dual-polarized antennas at 2.5 GHz," *IEEE Trans. Wireless Commun.*, vol. 3, no. 6, pp. 2288–2298, Nov. 2004.

[20] L. Schumacher, K. I. Pedersen, and P. E. Mogensen, "From antenna spacings to theoretical capacities—Guidelines for simulating MIMO systems," in *Proc. 13th Pers., Indoor Mobile Radio Commun.*, Sep. 2002, pp. 587–592.

[21] Y. S. Cho, J. Kim, W. Y. Yang, and C. G. Kang, *MIMO-OFDM Wireless Communication Technology With MATLAB*. Beijing, Germany: Publishing House Electron. Ind., 2013.

[22] J. D. Parsons and A. M. D. Turkmani, "Characterisation of mobile radio signals: Model description," *IEE Proc. I Commun., Speech Vis.*, vol. 138, no. 6, pp. 549–556, Dec. 1991.

[23] C. Oestges, "A comprehensive model of dual-polarized channels: From experimental observations to an analytical formulation," in *Proc. IEEE 3rd Int. Conf. Commun. Netw.*, Aug. 2008, pp. 1071–1075.

[24] L. Jiang, L. Thiele, and V. Jungnickel, "On the modelling of polarized MIMO channel," in *Proc. IEEE Eur. Wireless Conf.*, Apr. 2007, pp. 1–6.

[25] Y. Ma, Z. Zheng, and Y. L. Zhou, "Characteristics of MIMO channel in consideration of polarization," in *Proc. Wireless Commun., Netw. Mobile Comput.*, 2009, pp. 1–3.

[26] G. J. Foschini and M. J. Gans, "On limits of wireless communications in a fading environment when using multiple antennas," *Wireless Pers. Commun.*, vol. 6, no. 3, pp. 311–335, Mar. 1998.

[27] P. Soma, D. S. Baum, V. Erceg, R. Krishnamoorthy, and A. J. Paulraj, "Analysis and modeling of multiple-input multiple-output (MIMO) radio channel based on outdoor measurements conducted at 2.5 GHz for fixed BWA applications," in *Proc. IEEE Int. Conf. Commun. (ICC)*, May 2002, pp. 272–276.

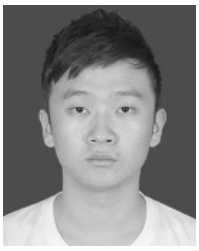

**XUDONG CHENG** received the B.S. degree in communication engineering from Shenzhen University, China, in 2013, where he is currently pursuing the Ph.D. degree with the College of Information Engineering. His current research interests include channel modeling, especially polarized MIMO channel modeling, energy harvesting communications, smart antennas, and signal processing.

**YEJUN HE** (SM'09) received the Ph.D. degree in information and communication engineering from the Huazhong University of Science and Technology, Wuhan, China, in 2005. From 2005 to 2006, he was a Research Associate with the Department of Electronic and Information Engineering, The Hong Kong Polytechnic University, Hong Kong. From 2006 to 2007, he was a Research Associate with the Department of Electronic Engineering, Faculty of Engineering, The Chinese University of Hong Kong, Hong Kong. In 2012, he was a Visiting Professor with the Department of Electrical and Computer Engineering, University of Waterloo, Waterloo, ON, Canada. From 2013 to 2015, he was an Advanced Visiting Scholar (Visiting Professor) with the School of Electrical and Computer Engineering, Georgia Institute of Technology, Atlanta, GA, USA. Since 2011, he has been a Full Professor with the College of Information Engineering, Shenzhen University, Shenzhen, China, where he is currently the Director of the Guangdong Engineering Research Center of Base Station Antennas and Propagation, and the Director of the Shenzhen Key Laboratory of Antennas and Propagation, Shenzhen, China. He has authored or co-authored over 100 research papers, books (chapters), and holds 13 patents. His current research interests include channel coding and modulation, 4G/5G wireless mobile communication, space-time processing, antennas and RF. He is a Fellow of IET. He has also served as a Technical Program Committee Member or a Session Chair for various conferences, including the IEEE Global Telecommunications Conference, the IEEE International Conference on Communications, the IEEE Wireless Communication Networking Conference, and the IEEE Vehicular Technology Conference. He is the Principal Investigator for over 20 current or finished research projects, including NSFC of China, the Integration Project of Production Teaching and Research by Guangdong Province and Ministry of Education and the Science and Technology Program of Shenzhen City. He has served as a Reviewer for various journals, such as the IEEE TRANSACTIONS ON VEHICULAR TECHNOLOGY, the IEEE TRANSACTIONS ON COMMUNICATIONS, the IEEE TRANSACTIONS ON WIRELESS COMMUNICATIONS, the IEEE TRANSACTIONS ON INDUSTRIAL ELECTRONICS, the IEEE WIRELESS COMMUNICATIONS, the IEEE COMMUNICATIONS LETTERS, the IEEE JOURNAL ON SELECTED AREAS IN COMMUNICATIONS, *International Journal of Communication Systems*, *Wireless Communications and Mobile Computing*, and *Wireless Personal Communications*. He is currently serving as an Associate Editor of the IEEE ACCESS and *Security and Communication Networks*.

**MOHSEN GUIZANI** (S'85–M'89–SM'99–F'09) received the B.S. (Hons.) and M.S. degrees in electrical engineering, and the M.S. and Ph.D. degrees in computer engineering from Syracuse University, Syracuse, NY, USA, in1984, 1986, 1987, and 1990, respectively. He served as the Associate Vice President of Graduate Studies, Qatar University, the Chair of the Computer Science Department, Western Michigan University, and the Chair of the Computer Science Department, University of West Florida. He also served in academic positions at the University of Missouri–Kansas City, University of Colorado Boulder, Syracuse University, and Kuwait University. He is currently a Professor and the ECE Department Chair with the University of Idaho, USA. He is the author of nine books and over 450 publications in refereed journals and conferences. His current research interests include wireless communications and mobile computing, computer networks, mobile cloud computing, security, and smart grid. He is a Senior Member of ACM. He also served as a member, the Chair, and the General Chair of a number of international conferences. He received the teaching award multiple times from different institutions and the Best Research Award from three institutions. He was the Chair of the IEEE Communications Society Wireless Technical Committee and the Chair of the TAOS Technical Committee. He served as the IEEE Computer Society Distinguished Speaker from 2003 to 2005. He guest edited a number of special issues in IEEE journals and magazines. He currently serves on the editorial boards of several international technical journals and the Founder and the Editor-in-Chief of *Wireless Communications and Mobile Computing Journal* (Wiley).